Journal of Marine Science and Application (2026) 25: 259-276
https://doi.org/10.1007/s11804-025-00640-5

RESEARCH ARTICLE

Carbon Footprint and Economic Analysis of LNG-fueled Fishing Vessel Using Real Engine Performance Simulation

Momir Sjerić[1], Maja Perčić[1], Ivana Jovanović[1] and Nikola Vladimir[1]

Received: 16 October 2024 / Accepted: 24 December 2024

Abstract

Analysis of the environmental and economic performance of fishing vessels has received limited attention compared with other ship types despite their notable contribution to global greenhouse gas (GHG) emissions. This study evaluates the carbon footprint (CF) and economic viability of a liquefied natural gas (LNG) -fueled fishing vessel, using real engine operation simulations to provide precise and dynamic evaluation of fuel consumption and GHG emissions. Operational profiles are obtained through the utilization of onboard monitoring systems, whereas engine performance is simulated using the 1D/0D AVL Boost™ model. Life cycle assessment (LCA) is conducted to quantify the environmental impact, whereas life cycle cost assessment (LCCA) is performed to analyze the profitability of LNG as an alternative fuel. The potential impact of the future fuel price uncertainties is addressed using Monte Carlo simulations. The LCA findings indicate that LNG has the potential to reduce the CF of the vessel by 14% to 16%, in comparison to a diesel power system configuration that serves as the baseline scenario. The LCCA results further indicate that the total cost of an LNG-powered ship is lower by 9.5%–13.8%, depending on the share of LNG and pilot fuels. This finding highlights the potential of LNG to produce considerable environmental benefits while addressing economic challenges under diverse operational and fuel price conditions.

Keywords 1D/0D simulation; Carbon footprint; Fishing vessels; Life cycle assessment; Life cycle cost assessment; Liquefied natural gas

1 Introduction

Currently, one of the most important environmental challenges is global warming, which represents the long-term increase in the Earth's average surface temperature because of human activities, primarily the overuse of fossil fuels, resulting in increased greenhouse gas (GHG) emissions into the atmosphere. These emissions refer to carbon dioxide (CO_2, as the main GHG), methane (CH_4), nitrous oxide (N_2O), and fluorinated gases (at low concentrations). These emissions form a dense layer in the atmosphere that traps heat through the greenhouse effect, thereby contributing to global warming and climate change (UNFCCC, 2001). According to the Paris Agreement, significant decarbonization should be achieved across all sectors of human activity to solve the problem of global warming (UNFCCC, 2024).

Ships primarily use fossil fuels, such as heavy fuel oil or marine diesel oil, for propulsion, thus releasing large amounts of CO_2, sulfur oxides, and nitrogen oxides (NO_x) into the atmosphere (Jovanović et al., 2022). According to the International Maritime Organization (IMO), the shipping sector is responsible for approximately 3% of global CO_2 emissions (IMO, 2020). As global trade continues to grow, these emissions are expected to increase, making decarbonization efforts crucial (Perčić et al., 2022). To address these challenges, in 2023, IMO adopted the Strategy on Reduction of GHG Emissions from Ships, which provides a framework for mid- and long-term decarbonization measures, timelines, and expected impacts. By 2030, international shipping must reduce total annual GHG emissions by at least 20% (target of 30%), reduce carbon intensity by at least 40% compared with the 2008 levels, and ensure that at least 5% (target of 10%) of energy use comes from zero or near-zero GHG emission sources (IMO, 2023). These targets are achievable through the implementation of vari-

Article Highlights

- The study evaluates an LNG-fueled fishing vessel's environmental and economic performance using real engine operation simulations.
- LCA results demonstrate that LNG reduces the vessel's carbon footprint by 14%–16% compared to diesel as a baseline scenario.
- LCCA reveals that LNG-powered ship reduces total costs by 9.5%–13.8% compared to the diesel-powered ship.
- Monte Carlo simulations address the impact of future fuel price uncertainties on the economic viability of LNG.

✉ Nikola Vladimir
nikola.vladimir@fsb.unizg.hr

[1] Faculty of Mechanical Engineering and Naval Architecture, University of Zagreb, Ivana Lučića, 510000 Zagreb, Croatia

ous technical and operational measures to reduce emissions (Bouman et al., 2017; Karatug et al., 2022).

An important measure to reduce shipping emissions is replacing conventional marine fuels with alternative, cleaner energy sources. These alternatives can be low-carbon fuels (e.g., liquefied natural gas (LNG) and methanol), carbon-neutral fuels (e.g., biofuels and e-fuels), or zero-carbon fuels (e.g., hydrogen, ammonia, and electricity) (Perčić et al., 2023a). The shipping industry is gradually adopting these alternative fuels, marking a significant step toward a low-carbon future. A key indicator of that is the order book for new ships. According to order data from 2023, approximately 23% of newly ordered ships will be powered by alternative fuels (DNV, 2023).

The viability of utilizing alternative fuels in the shipping industry is frequently evaluated through life cycle assessment (LCA), which assesses the environmental impact and footprint of vessels operating with alternative fuels (Blanco-Davis and Zhou, 2014). In addition, economic analyses, such as life cycle cost assessment (LCCA), are employed to evaluate the profitability of these alternative solutions compared with conventional power options (Kjær et al., 2015). Researchers frequently compare alternative marine fuels based on their environmental footprint. For example, Bilgili (2021) conducted an LCA to evaluate the environmental impact of various alternative marine fuels, including biogas, dimethyl ether, ethanol, LNG, liquefied petroleum gas (LPG), methanol, ammonia, and biodiesel. Their assessment covered multiple impact categories, such as human health, ecosystems, resource use, emissions, and social costs. A comparable study was conducted by Tomos et al. (2024), in which LCA was employed to evaluate the environmental impact of diverse alternative fuels in accordance with the annual propulsion energy requirements of the global fleet. However, these studies did not include case studies of actual operating ships. In this context, several researchers have concentrated their efforts on LCA, LCCA, or a combination of the two, with a particular focus on single fuels used onboard specific vessels. For instance, Wang et al. (2021) explored the use of an all-electric ferry, whereas Kim et al. (2023) investigated the potential of LPG-powered fishing vessels. Several researchers have examined a range of alternative fuels in use on specific vessels, evaluating their performance in comparison to existing alternative propulsion systems (Ha et al., 2023; Huang et al., 2022; Korberg et al., 2021; Koričan et al., 2022; Perčić et al., 2020a; Wang et al., 2020).

Among various alternative marine fuels, methanol and LNG are highlighted as the most investigated and mentioned alternative fuels. This focus on methanol and LNG is reflected in the recent trends in the shipping industry: In 2023, 298 ships with alternative propulsion systems were placed on order, marking an 8% increase compared with the previous year. Methanol drew significant interest with 138 ships ordered, positioning it alongside LNG with 130 ships ordered. LNG has been predominantly used on new builds for years; however, the increasing orders for methanol-powered ships indicate its growing prominence as an alternative fuel in the maritime sector (DNV, 2023). Both LNG and methanol represent promising alternative marine fuels, each having distinct advantages and challenges. LNG propulsion is a mature technology, and LNG has a higher energy density than methanol, resulting in smaller storage requirements. However, LNG requires cryogenic storage and can result in CH_4 slip, a potent GHG (Kumar et al., 2011; Yao et al., 2023). Methanol, although more straightforward to store and handle at ambient temperatures, has a lower energy density than LNG, necessitating larger storage volumes and a less developed infrastructure (Ammar, 2019; Qu et al., 2023). A significant number of researchers have conducted investigations into the potential applications of LNG in the maritime sector. These investigations have primarily employed LCA and LCCA methodologies. The findings of these investigations have generally concluded that LNG serves as a transitional fuel with the capacity to reduce emissions and promote greener shipping practices. Furthermore, the implementation of carbon credit mechanisms has been identified as a means of enhancing the potential of LNG as a viable and attractive option during the transition toward sustainable shipping solutions (Butarbutar et al., 2023; Jang et al., 2021; Karatuğ et al., 2023a; Taghavifar and Perera, 2023a; Taghavifar and Perera, 2023b).

Nevertheless, a comprehensive assessment of test cases requires precise data on fuel consumption (FC) to calculate the environmental impact of the ship during operation and evaluate its economic performance because fuel costs represent a significant expense over the lifetime of a ship. Furthermore, the performance and efficiency of alternative powering solutions are subject to several additional factors, including real-world operational practices, schedules, maintenance requirements, and unexpected demands. These factors are often overlooked in current studies on alternative marine fuels.

1.1 Carbon footprint assessment in the shipping sector

Carbon footprint (CF) is defined as the total quantity of CO_2 or all GHG emissions released directly or indirectly by human activities (Yan et al., 2023). The assessment of the CF of a ship has been a pivotal area of investigation in maritime research largely because of the rigorous regulations and the imperative for exploring alternative power sources. Typically, CF is calculated based on the FC of the vessel.

Most studies in this domain have predominantly relied on theoretical models, controlled experiments, or limited field data. Hulskotte and Denier van der Gon (2010) conducted an onboard survey of energy consumption and fuel use on ships to estimate emissions from vessels at berth. This approach provided valuable insights into emissions during specific operational phases but was limited to static conditions and did not account for the dynamic nature of ship operations. Jeong et al. (2020) introduced a methodology for calculating the CF of small ships by simulating potential changes in operating conditions, such as speed, time, and displacement. Although this method advanced the understanding of CF by considering variable operational profiles, it remained dependent on estimated operational profiles rather than real-world data. This dependence introduces uncertainties, as actual vessel operations often deviate from estimated profiles because of a range of factors, including weather conditions and navigational requirements. Ančić et al. (2020) employed a bottom-up approach to evaluate the CF of ships powered by conventional power systems, focusing on the Croatian ferry fleet. Their method considered schedule, distance, duration, and power–speed correlation but did not account for the specific power capabilities of individual vessels. As a result, their approach provided a generalized CF estimate that might not accurately reflect the diverse operational characteristics of different ships. To address this limitation, Perčić et al. (2020b) refined the methodology by incorporating the assumed loads of the main and auxiliary engines to calculate energy requirements and using fixed specific FC to calculate FC. They further conducted an LCA to evaluate the environmental impact of alternative power systems on board Croatian ferries, providing a more holistic view of the environmental implications. A similar study was conducted by Perčić et al. (2021) for inland navigation vessels. Karatuğ et al. (2023b) investigated the environmental and economic performance of an LNG-powered container vessel using FC data from noon reports collected over a year. The novelty of their study lies in conducting economic analyses under various FC scenarios while addressing uncertainties through the Monte Carlo simulation approach, highlighting the significant emission reductions of LNG compared with very low sulfur fuel oil and marine gas oil. However, the economic viability of LNG remains highly sensitive to fluctuations in fuel prices. Zhou et al. (2024) introduced CF assessment of inland vessels by implementing a voyage-based carbon emissions accounting framework. They calculated emissions using data on main engine operation, load, operating time, and carbon factors and provided a more detailed assessment of emissions by categorizing voyages into loading, transit, and unloading stages. Although their study improved the accuracy of emissions data by leveraging operational details, it did not fully capture the complexities of real-time engine performance under varying conditions. This limitation is particularly critical because the operational profiles of ships are subject to numerous variables, including speed, load, and other operational factors. These variables can lead to substantial variations in the CF of a vessel compared with those derived from idealized or laboratory conditions (Jang et al., 2024).

The performance of marine engines can be evaluated using physical and intelligent simulation tools. Physical simulation tools, such as GT-Power, Ricardo WAVE, and AVL Boost™, are widely used to simulate engine performance at various speeds and loads, using numerical models of varying complexity to analyze and optimize engine performance. By contrast, intelligent simulation tools are based on data-driven models, which can be divided into statistical and machine-learning-based approaches (Karatuğ et al., 2024). These models are commonly used in maritime research to predict ship performance and FC, especially in complex marine environments. Typically applied to individual ships, data-driven models require large datasets to ensure the accuracy and reliability of predictions (Guo et al., 2022). Many researchers conducted simulations of marine engines, including diesel engines (Taghavifar and Mazari, 2022; Xin et al., 2022) and dual-fuel engines (Theotokatos et al., 2020; Taghavifar, 2023). However, these studies did not incorporate real-time simulations of ship engine operations during the ship route. Ghorbani et al. (2023) developed a numerical simulation tool to evaluate the performance of a wind-assisted container ship on real routes. Their model incorporated the dynamics of the hull, rudder, controllable pitch propeller, main engine FC, and suction sail force. Developed in-house in Python, their tool was based on a generic 4-degree-of-freedom cargo ship model. The accuracy of their tool was validated with onboard sensor data from short-distance and long-distance voyages. In their study, Karatuğ et al. (2024) presented a decision support system for improving ship energy efficiency using real-time data from noon reports. Their engine optimization model for the container ship was developed by combining Ricardo WAVE software and a nonlinear optimizer integrated into MATLAB. Meanwhile, an artificial neural network estimated the FC. Sjerić et al. (2024) employed a one-dimensional/zero-dimensional (1D/0D) simulation model using AVL Boost™ to calculate the engine FC and NO_x and soot emissions of a container ship. Their study aimed to determine the optimal sailing speed under slow steaming conditions by evaluating the trade-off between reduced fuel costs and CO_2 and NO_x emissions and increased operating costs in light of recent legislative measures to reduce shipping emissions.

The aforementioned studies provided significant insights into the operational dynamics of marine engines on specific vessels, particularly on container ships with well-defined operational profiles. These ships follow fixed routes and schedules, operating at consistent speeds and power requirements. However, fishing vessels operate under highly variable conditions, frequently adjusting their routes, speed, and power requirements based on fishing conditions, weather, and availability. This variability results in operational profiles that are more difficult to predict, with power requirements indicating considerable fluctuations across the various phases of fishing operations (FAO, 2021), which emphasizes a significant research gap in the comprehension of the genuine operational profiles and CF of fishing vessels, particularly when alternative fuels are utilized.

Moreover, the emission reduction measures are primarily directed at long-distance and short-distance shipping. Meanwhile, fishing vessels remain largely overlooked despite their contribution to shipping emissions. The total annual FC of the global fishing fleet is estimated at approximately 40 billion liters, resulting in 179 million tons of CO_2 equivalent (CO_2-eq), which corresponds to approximately 2.2 tons of CO_2-eq per ton of landed fish (Baiju et al., 2024). The fishing sector mostly comprises older vessels that operate with outdated engines, generating high levels of harmful emissions released into the atmosphere. In addition, their varying operating regimes can lead to increased emissions. Moreover, these ships spend a long time near the port and polluted areas, directly affecting the air quality of the local population (Koričan et al., 2023; Liu et al., 2018; Szelangiewicz et al., 2021).

1.2 Aim of the study

Although fishing vessels are not bound by IMO regulations on emission reduction, their impact on global warming should not be neglected. The number of studies examining alternative marine fuels for fishing vessels is limited in comparison to other ship types. In a study conducted by Perčić et al. (2023b), the potential for alternative fuels in a Croatian fishing vessel (purse seiner) was investigated through a combination of LCA and LCCA. Nevertheless, their study was deficient in the absence of genuine engine operation simulations and an evaluation of the actual FC.

The objective of this study is to address the aforementioned gap by employing real-time simulations of engine operation, thereby enabling a more precise and dynamic evaluation of FC and CF for fishing vessels powered by conventional fuels and LNG, which is one of the most widely used alternative fuels in ships worldwide. The simulation of real engine operations, resulting in precise FC and CF during ship operation, is conducted using the 1D/0D AVL Boost™ model, which utilizes real-time data from the onboard monitoring system. To evaluate the environmental impact of the proposed replacement on the specific ship, an LCA is conducted, which is complemented by an LCCA to evaluate the profitability of the proposed replacement. Meanwhile, future fuel price uncertainties are analyzed using Monte Carlo simulations to account for current price fluctuations.

The real contribution of this research lies in its approach to directly simulate the operation of the engine of a fishing vessel, capturing the environmental impact during a typical operating cycle using actual measured data. In contrast to previous studies that rely on emission indices and theoretical energy estimates based on installed power, this work provides a more accurate and detailed assessment of emissions and energy consumption by incorporating real-world operational data.

2 Methodology

2.1 Ship particulars and operative profiles

The diversity of fishing vessels is reflected in their varying sizes and the gear types that they utilize, which determines the species they catch and the fishing activities they are capable of. Approximately 86% of all motorized global fishing vessels are shorter than 12 m in length, whereas less than 2% of industrial fishing vessels, such as purse seiners, are longer than 24 m in length and exceed 100 gross tonnage (GT) (FAO, 2021). In Croatia, although there are not many purse seiners in the fishing fleet, they are responsible for 55% of the landing value and 90% of the landing weight (Ministry of Agriculture of the Republic of Croatia, 2023). In this study, the Croatian purse seiner is investigated, Figure 1, and its main particulars are presented in Table 1.

Figure 1 Fishing vessel “Briljant”

Table 1 Fishing vessel data (Ministry of Agriculture of Republic of Croatia, 2023)

Name	Briljant
Ship type	Purse seiner
Year of production	1967
Length overall (m)	32.28
Breadth (m)	7.4
Draught (m)	2.88
GT	182
Max. speed (kn)	11

The vessel is propelled by a Mitsubishi S6R2-T2MPTK four-stroke diesel engine, and its main parameters and performance are specified in Table 2. The engine is equipped with a turbocharger (TC) and intercooler element (CO), producing the maximum brake power of 640 kW at an engine speed of 1 500 r/min. According to the engine manufacturer data, the engine satisfies the IMO II standard related to the maximum NO_x emissions.

Table 2 Engine data and performance

Engine	Mitsubishi S6R2-T2MPTK
Type	4-stroke, water-cooled
Aspiration	Turbocharger, intercooler element
Cylinder arrangement	Inline
No. of cylinders	6
Cylinder bore (mm)	170
Piston stroke (mm)	220
Compression ratio	14
No. of valves	2 intake, 2 exhaust
Moment of inertia of rotating components ($kg{\cdot}m^2$)	11.96
Idling speed (r/min)	600–650
Maximum overspeed capacity (r/min)	1 750
Maximum brake power	640 kW at 1 500 r/min
Brake power	D rating = 610 kW at 1 500 r/min C rating = 530 kW at 1 400 r/min B rating = 480 kW at 1 350 r/min
Engine International Air Pollution Prevention (EIAPP)	IMO II

The operational profile of a typical purse seiner encompasses a series of activities, including cruising to the open sea, searching for fish, encircling the fish (setting the net), hauling, loading, and cruising back to port. These activities are subject to significant daily fluctuations, with alterations in fishing locations, weather conditions, and operational strategies resulting in notable fluctuations in FC (Perčić et al., 2023b). To accurately determine the actual FC and associated CF, the specific operating regime of a vessel needs to be investigated (Basurko et al., 2016). Several Croatian fishing vessels, including the one observed, are equipped with FC monitoring systems, global positioning system (GPS) tracking, and accessory switches that indicate engine activation or deactivation. These systems are linked to the MAPON software (MAPON, 2024), which provides real-time data on the activities, routes, specific locations, fuel use, and speed of the vessel (Koričan et al., 2023) (Figure 2).

2.2 Simulation of real engine operational performance

To gain insights into the actual FC and CF of the analyzed vessel, a simulation of the real operational performance of the engine is conducted. In the first step, the engine simulation model in AVL Boost™ was calibrated over the load speed data at a constant engine speed of 1 500 r/min. The load sweep data were defined by the engine manufacturer and corresponded to 25%, 50%, 75%, and 100% of the engine load. The simulation results under steady operating conditions for engine torque and brake-specific fuel consumption (BSFC, g/kWh) were compared with the reference data. The combustion timing and scaling factor for cylinder heat losses were calibrated to achieve a maximum difference between simulated and reference data of ±3%.

In the second step, the simulation of a conventional fishing vessel propulsion system was performed over a typical operating regime obtained using the MAPON software

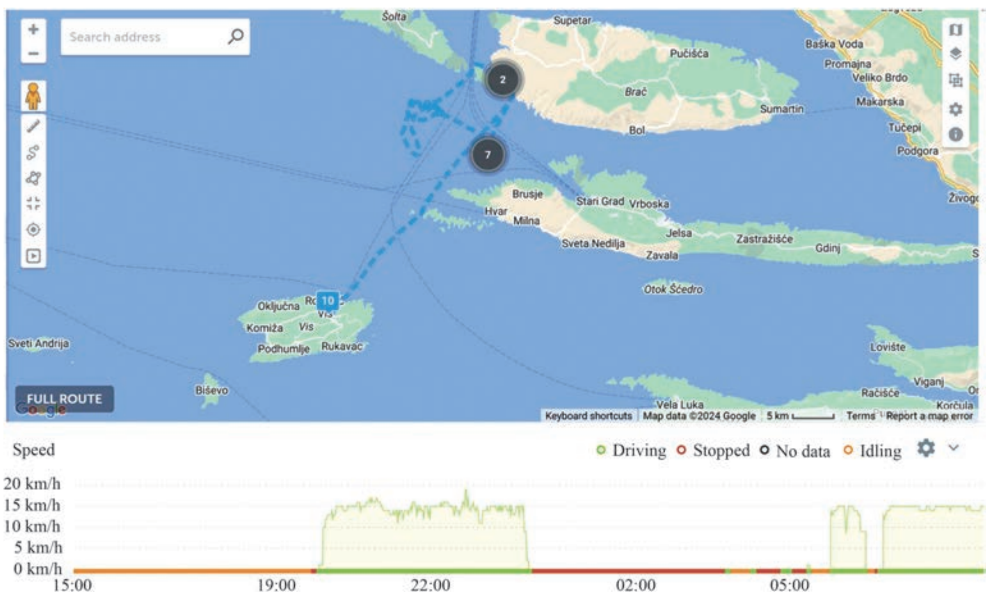

Figure 2 Real-time data preview from the MAPON software

that has dynamic features with initial and final transition periods of approximately 5–10 min and average speeds of approximately 13–14 km/h. The observed fishing cycle lasted for a total of 293 min. Once the engine control unit (ECU) element of the simulation model has been correctly adjusted to control the injected fuel per cycle for the original engine, the simulation of engine operation is performed. The integration of total injected fuel mass resulted in total consumed fuel mass.

In the third step, the engine simulation model was upgraded to operate under the conventional dual-fuel operation. The LNG fuel injectors were added to the intake ports, and the ECU controlled the fuel mass injection. This study investigated three combinations of LNG and diesel fuel: 85% LNG with 15% diesel, 90% LNG with 10% diesel, and 95% LNG with 5% diesel. The properties of the fuel used in the dual-fuel mode were defined using the Boost gas property tool, taking into account different mass fractions of LNG and diesel. The dual-fuel engine operation was simulated over the same fishing vessel operating regimes.

The ship propulsion system is modeled using the comprehensive thermodynamic cycle simulation model of AVL Boost™, which is a virtual engine simulation software for accurately predicting engine performance and emissions under steady and unsteady operating conditions (Bellér et al., 2021). The flow through the intake and exhaust pipes is calculated as 1D flows with the finite volume method. The cylinder is considered to have one control volume that changes over time as the piston moves between dead centers. Therefore, this approach is usually called 0D. Two min equations, namely mass conservation and energy equations, are calculated for the cylinder at each time step. The change in in-cylinder mass is calculated as follows:

$$\frac{\mathrm{d}m_C}{\mathrm{d}\alpha} = \sum \frac{\mathrm{d}m_i}{\mathrm{d}\alpha} - \sum \frac{\mathrm{d}m_e}{\mathrm{d}\alpha} - \frac{\mathrm{d}m_{\mathrm{BB}}}{\mathrm{d}\alpha} + \frac{\mathrm{d}m_{\mathrm{ev}}}{\mathrm{d}\alpha} \tag{1}$$

where m_C is the total in-cylinder mass. The first term on the right-hand side is the intake mass flow, the second term is the exhaust mass flow, the third term is the blow-by mass flow (between piston rings and cylinder liner), and the last term is related to the mass flow of fuel directly injected into the cylinder. To calculate the change in in-cylinder temperature, the derivative of the energy equation is calculated as follows:

$$\frac{\mathrm{d}(m_C \cdot u)}{\mathrm{d}\alpha} = -p_C \cdot \frac{\mathrm{d}V}{\mathrm{d}\alpha} + \frac{\mathrm{d}Q_F}{\mathrm{d}\alpha} - \sum \frac{\mathrm{d}Q_W}{\mathrm{d}\alpha} - h_{\mathrm{BB}} \cdot \frac{\mathrm{d}m_{\mathrm{BB}}}{\mathrm{d}\alpha} + \sum \frac{\mathrm{d}m_i}{\mathrm{d}\alpha} \cdot h_i - \sum \frac{\mathrm{d}m_e}{\mathrm{d}\alpha} \cdot h_e - q_{\mathrm{ev}} \cdot f \cdot \frac{\mathrm{d}m_{\mathrm{ev}}}{\mathrm{d}\alpha} \tag{2}$$

where u is the specific internal energy, p_C is the in-cylinder pressure, and V is the total cylinder volume. The second term $\frac{\mathrm{d}Q_F}{\mathrm{d}\alpha}$ is the rate of heat release, the third term $\frac{\mathrm{d}Q_W}{\mathrm{d}\alpha}$ is the heat flow through walls, and the fourth, fifth, and sixth terms are related to the enthalpy flows of blow-by, intake, and exhaust, respectively. The last term takes into account the change in in-cylinder energy caused by the evaporation process typical for the injection of liquid fuels.

The rate of heat release is proportional to the instantaneous rate of burning fuel $\frac{\mathrm{d}x}{\mathrm{d}\alpha}$, calculated as follows:

$$\frac{\mathrm{d}Q_F}{\mathrm{d}\alpha} = \mathrm{LHV} \cdot m_{f,\,\mathrm{cycle}} \cdot \frac{\mathrm{d}x}{\mathrm{d}\alpha} \tag{3}$$

where LHV is the lower heating value of applied fuel and $m_{f,\,\mathrm{cycle}}$ is the total fuel mass per operating cycle. The mass ratio of fuel burned is calculated by adopting the well-known Vibe function as follows:

$$x(\alpha) = \frac{m_f(\alpha)}{m_{f,\,\mathrm{cycle}}} = 1 - \mathrm{e}^{-6.9\left(\frac{\alpha}{\alpha_{\mathrm{comb}}}\right)^{m+1}} \tag{4}$$

where α_{comb} is the predefined combustion duration, and m is the shape parameter influencing the instantaneous combustion progress. Typical values of shape parameters for the combustion process governed by diffusion flame in a compression ignition engine are from 0.4 to 1.1. Meanwhile, for flame propagation, which is typical for spark ignition engines, the shape parameter ranges from 1.9 to 2.6 (AVL Boost, 2013). The simulation of the original diesel engine was performed with the Vibe shape parameter set as 1.0. Meanwhile, in the dual-fuel combustion model, the shape parameter was set to 2.0 because flame propagation is expected to be the dominant combustion mode. In both simulation models, the combustion duration was set to 65° crank angle (CA), whereas the start of combustion was varied from 5° CA before top dead center (BTDC) at low engine speed to 15° CA BTDC at maximum engine speed.

In this study, the full simulation model of the engine of a fishing vessel was generated using AVL Boost™ version 2013.2, as shown in Figure 3.

The engine intake system is described from the system boundary 1 (SB1) element to the intake ports defined by pipe elements 5–10. The engine is equipped with TC1 and CO1. The exhaust system starts from the exhaust ports defined by pipe elements 11–17 to SB2, where exhaust gases flow out to the environment. The engine element (E1) defines the firing order, engine friction, and engine inertia required for transient engine operation. The vehicle element (V1) is connected via mechanical connection to the engine, representing the direct connection of the vessel propeller to the engine crankshaft. The vehicle element data include vehicle load characteristics, mass, and desired vehicle velocity table that is typical for the operational profile of each vessel. Conventional dual-fuel operation can

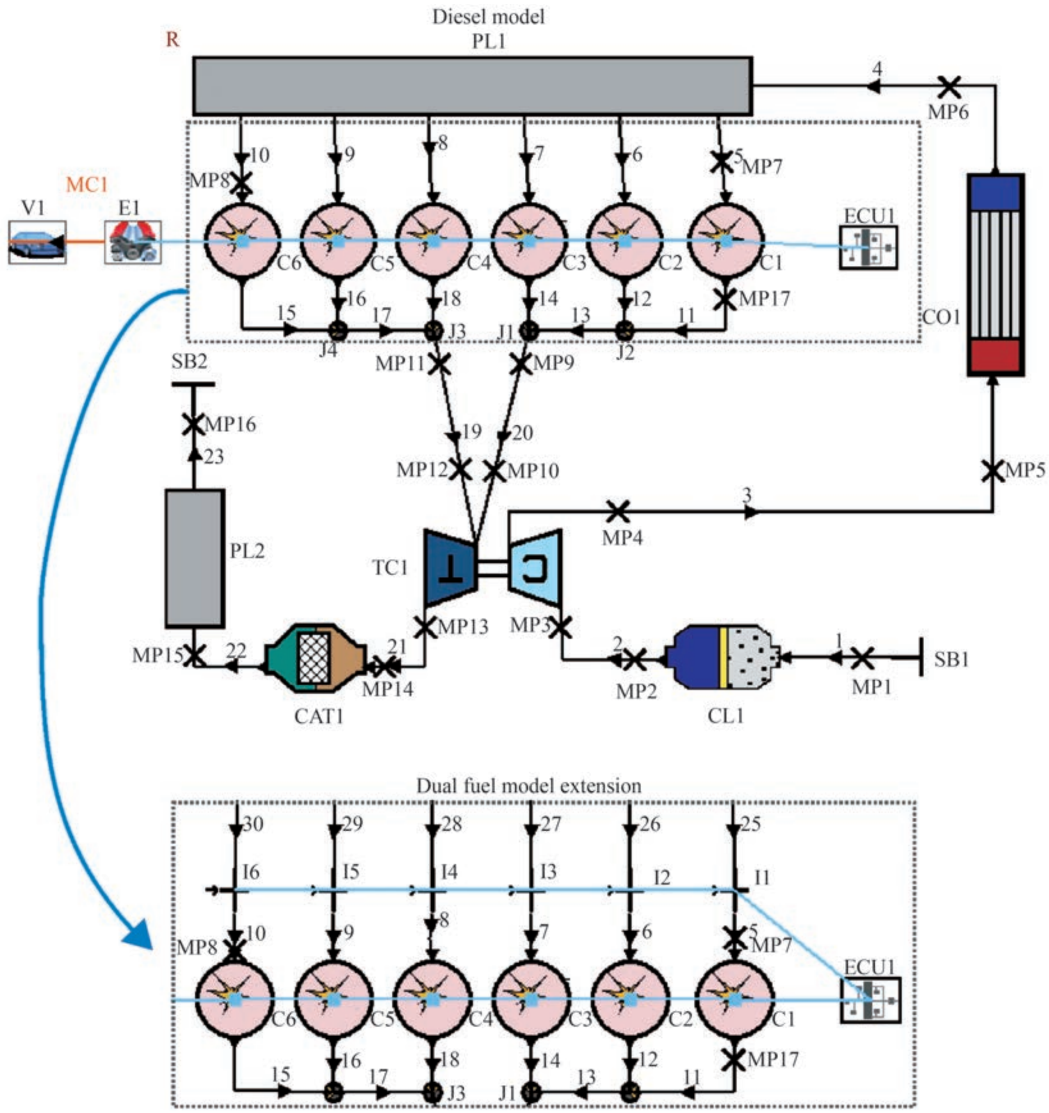

Figure 3 1D/0D simulation model of the original diesel and dual-fuel propulsion systems

be achieved with the installation of low-pressure LNG injectors at the intake ports (pipe elements 5–10), creating the premixed mixture of LNG and air that enters the cylinder during the intake, as shown in Figure 3. The ECU1 is applied to control the energy of fuel delivered to the cylinders depending on the instantaneous engine load. In the case of diesel engine operation, the ECU element controls the mass of fuel directly injected into each cylinder. At a maximum engine load equal to 100%, the maximum fuel quantity of 0.49 g/cycle is injected at each cylinder. By contrast, at an engine load of 0%, fuel is not added. For engine loads between 0% and 100%, the ECU element performs linear interpolation. When the dual-fuel engine operation is simulated, the ECU element is connected to the port fuel injectors (I1–I6) added to the intake pipes, as shown in Figure 3. At an engine load of 100%, the maximum fuel amount of 0.42 g/cycle is injected at each intake port.

In dual-fuel combustion mode, the combustion process is initiated by the direct injection of a small amount of diesel fuel around the top dead center. Because two different fuels cannot be defined separately in the applied simulation model, the Boost gas property tool was used to define the fuel properties when LNG and diesel fuel are mixed. The overview of diesel, LNG, and dual fuel considered in this study is given in Table 3.

The simulation results of the FC (kg) of the purse seiner for a typical fishing cycle are obtained. To perform further analysis of the environmental and economic impact of different power systems on board the vessel, the annual FC (FC_A, kg) needs to be calculated, which is achieved by multiplying the number of working hours per year by the hourly FC. In a study conducted by Koričan et al. (2023), the operational patterns of several Croatian purse seiners and trawlers were analyzed using the MAPON software. The researchers discovered that the main engines of purse seiners operate for an average of 4 h daily. Considering the

Table 3 Fuel properties

Power system	Composition	LHV (MJ/kg)	A2F ratio (stochiometric) (kg/kg)	Molar mass (g/mol)	Carbon mass fraction
Diesel	$C_{10}H_{20} - C_{15}H_{28}$ = 75.0 vol% $C_6H_6 + C_8H_8$ = 25.0 vol%	42.80	14.70	226.45	0.862 5
LNG	CH_4 = 100.0%	50.04	17.22	16.04	0.748 6
Dual fuel	LNG = 85.0% (mass ratio) Diesel = 15.0% (mass ratio)	48.96	16.92	18.35	0.762 2
	LNG = 90.0% (mass ratio) Diesel = 10.0% (mass ratio)	49.32	17.02	17.51	0.757 7
	LNG = 95.0% (mass ratio) Diesel = 5.0% (mass ratio)	49.68	17.12	16.74	0.753 2

limitations on work quotas and the periodic fishing suspensions for fish stock restoration, the annual operating time was set to 200 days.

To calculate CO_2 emission from the obtained FC, the following stoichiometric equation of carbon oxidation is considered:

$$1\ \text{kg C} + \frac{32}{12}\ \text{kg O}_2 \rightarrow \frac{44}{12}\ \text{kg CO}_2 \tag{5}$$

Equation (5) indicates that burning 1 kg of carbon will produce 44/12 kg of CO_2. Total CO_2 emissions listed in Table 5 for driving cycles are calculated using the following equation:

$$\text{CO}_2[\text{kg}] = \frac{44}{12} \cdot \text{Fuel consumption}[\text{kg}] \cdot \text{Carbon mass fraction} \tag{6}$$

where the carbon mass fraction for each applied fuel is specified in Table 3.

To investigate another GHG that contributes to global warming, this study considers CH_4 emissions in the context of CH_4 slip, defined as the unburnt fuel released with the exhaust gas into the atmosphere because of valve overlap and the operation of the engine with a premixed mixture of fuel and air in the cylinder. For diesel fuel combustion, the CH_4 slip is equal to zero because, during valve overlap, air and residual combustion products are generated in the engine cylinder.

2.3 Life cycle assessment

Although the simulation of engine operation indicated the emissions as a result of the operation of the ship, this study needs to gain insights into the environmental impact of different power systems from the life cycle perspective by performing LCA, which evaluates the life cycle GHG emissions released over the 25-year lifetime of the ship. The LCA of existing and alternative power options is conducted using the GREET software (GREET, 2022), which includes a comprehensive database that covers various fuels, stationary processes, and transportation processes throughout their life cycles. Although primarily designed for land-based transportation modes, the fuel application processes of the GREET software can be easily adapted to model ship power systems. The GREET software is widely recognized and frequently used to conduct LCAs of alternative marine fuels (Perčić et al., 2023a; Zincir and Arslanoglu, 2024; Lee et al., 2024).

The assessment considers emissions from the well-to-tank (WTT) and tank-to-wake (TTW) phases of the life cycle of the ship power system. The WTT phase refers to the emissions released throughout the fuel cycle, including the extraction of raw materials, transportation to the production facility, fuel production, and distribution to the tank in ports. By contrast, TTW emissions are released during the ship operation, i.e., fishing activities. The processes included in the LCA of a diesel-powered ship (which serves as a baseline scenario) and an LNG-powered ship are presented in Figure 4. Meanwhile, the distances for transportation processes are obtained from a study conducted by Perčić et al. (2023b).

The WTT phases for LNG and diesel involve several distinct processes. In the case of LNG, the process commences with the extraction of natural gas in Qatar. Subsequently, the extracted natural gas is liquefied on-site in Qatar to facilitate transportation. Then, LNG is transported over a distance of 7 000 km to Croatia, where it is distributed to the port from which the observed vessel is operating. By contrast, the WTT phase for diesel includes the extraction process of crude oil in the Middle East. Then, crude oil is transported to Croatia via tanker, covering a distance of 4 000 km. Upon arrival at the Croatian terminal, the oil is transferred to the refinery in Rijeka through an oil pipeline. At the refinery, the crude oil is first refined into diesel and then distributed to the pump in the port using a tank truck. The WTT emissions are calculated using the LCA software GREET, whereas the TTW emissions are obtained by simulating real engine operation. The total life cycle emissions E_j (kg) are determined by adding the emissions of specific gases j (CO_2 and CH_4) from each phase, i.e., WTT and TTW phases, according to the following equation:

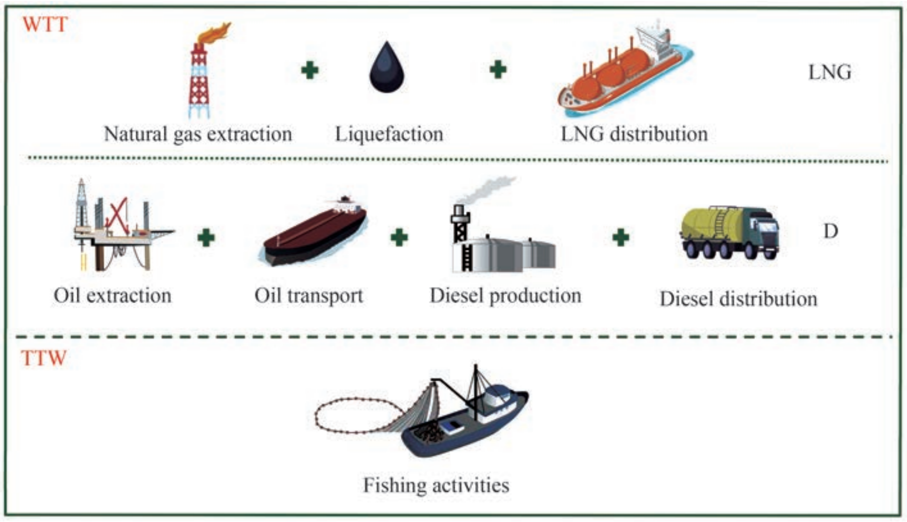

Figure 4 Processes included in the performed LCAs

$$E_j = E_{\text{WTT},\,j} + E_{\text{TTW},\,j} \tag{7}$$

The global warming potential (GWP, CO_2-eq) is used to assess the contribution of GHGs to global warming. GWP measures the amount of energy absorbed by a ton of a specific gas over a given time compared with the emission of a ton of CO_2. Using the CO_2-eq factors over 100 years (CO_2 : 1; CH_4 : 36), the CF can be calculated as follows (Perčić et al., 2022):

$$\text{GWP} = 1 \cdot E_{CO_2} + 36 \cdot E_{CH_4} \tag{8}$$

2.4 Life cycle cost assessment

The potential profitability of replacing diesel fuel with LNG on board fishing vessels is investigated through LCCA. This economic analysis considers the various types of costs associated with the ship power system over its 25-year lifetime, including both the capital cost (CapEx) and the ongoing operational costs (OpEx), i. e., maintenance cost, fuel cost, and carbon tax. This study compares the costs of different power systems using the net present value (NPV, €), which discounts future cash flows to their present value. The NPV of each power system is investigated with an assumed discount rate (r) of 5% and calculated as follows:

$$\text{NPV} = \text{CapEx} + \sum_{n=1}^{25} \frac{(\text{OpEx}_A)_n}{(1+r)^n} \tag{9}$$

where OpEx_A refers to the annual OpEx costs and n is the number of years of the ship's lifetime.

The investment cost of diesel-powered vessels is defined as the purchase price of a new engine, which is estimated at 180 €/kW (Perčić et al., 2023b). By contrast, the investment cost of LNG-powered vessels is significantly higher, i.e., at 1 290 €/kW, which includes the cost of a dual-fuel engine, an LNG storage tank, and other accompanying equipment (Lindstad et al., 2021). The maintenance costs of diesel and LNG are 0.014 and 0.015 €/kWh, respectively (Iannaccone et al., 2020). Fuel costs and carbon tax are defined in the subsequent subsections.

2.4.1 Monte carlo simulations

Fuel cost represents a significant expense over the lifetime of a ship. However, fuel cost is subject to considerable variation because of fluctuations in fuel prices resulting from, e. g., fluctuations in global crude oil prices or geopolitical events, such as the Russia – Ukraine conflict and the global COVID-19 pandemic (Duppati et al., 2023; Wu et al., 2024). Because of uncertainty regarding the fuel prices during the lifetime of the ship, future prices can be predicted by Monte Carlo simulations, which represent a highly accurate stochastic method that is employed for probabilistic uncertainty modeling. By conducting a substantial number of simulations, this method investigates the probability of different outcomes that are influenced by random variables, ensuring a comprehensive understanding of potential future scenarios (Colantoni et al., 2021; Bui et al., 2022).

This study investigates the prediction of future LNG and diesel fuel prices using the Monte Carlo simulations. As the simulation results depend on the quality of the inputs, comprehensive historical data on diesel and LNG prices need to be provided, as illustrated in Figure 5, which shows the average fuel prices over time.

The data on fluctuations in diesel prices over time was obtained by combining data from Statista (2024) and Tools (2024). Despite the exemption of the shipping sector in Croatia from excise duty on diesel, this study assumes the full price of diesel, given that subsidies will eventually come to an end and ship operators will be required to pay

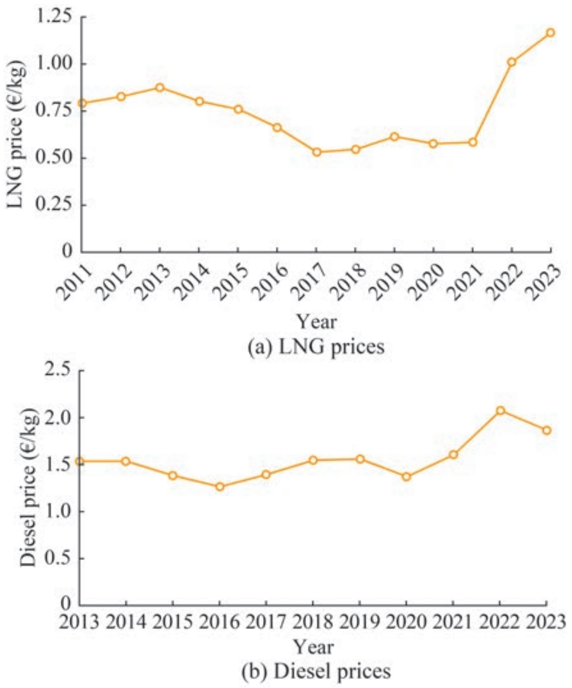

Figure 5 Fuel price fluctuations

the full price of their fossil fuel. In the absence of data on the price of LNG in Croatia, the price of natural gas in Croatia for non-household consumers has been used as a proxy (Eurostat, 2024; Trading Economics, 2024a). In addition, a global liquefaction price of 0.13 €/kg has been applied to this figure. This amount has been increased by 15% to account for the transportation costs associated with LNG (Zou et al., 2022).

The standard normal distribution is selected as the probability distribution, which is distinguished by its bell-shaped density curve. The standard normal distribution is a significant continuous probability distribution, defined by its mean and standard deviation (StDev), where extreme values in the dataset have a minimal impact on the mean value (Mishra et al., 2019). Furthermore, the Monte Carlo simulations entail the generation of random samples from the selected distribution using random number generators. The simulation is executed on multiple occasions to create a variety of potential outcomes.

2.4.2 Carbon tax

The implementation of a carbon tax in the shipping sector is designed to reduce GHGs by imposing a fee, i.e., carbon allowance, on CO_2 emissions released by ships during operation. This approach aims to incentivize the adoption of cleaner technologies and more efficient operational practices, thereby reducing the environmental impact of the sector (Bayraktar, 2023).

From January 2024, the EU's Emissions Trading System (EU ETS) has been expanded to include CO_2 emissions from large ships (5 000 GT and above) entering EU ports, irrespective of their flag. This study investigates the possibility of extending the EU ETS to other ship types, such as fishing vessels. To ensure a seamless transition to the additional costs, shipowners are required to pay for their reported emissions gradually. The initial payment will be 40% due in 2025, followed by 70% in 2026, and the final 100% in 2027 (European Commission, 2024). The current market price of CA (in December 2024) is approximately 66 €/t of CO_2 (Trading Economics, 2024b). However, the International Energy Agency (IEA) forecasts that this value could increase to 230 €/t of CO_2 by 2050. In their World Energy Outlook 2023 (IEA, 2023), three carbon pricing scenarios are presented, each with projected CA (€/t CO_2) for 2030, 2040, and 2050. These carbon pricing scenarios are the stated policies scenario (SPS), the announced pledges scenario (APS), and the net zero emissions by 2050 scenario (NZES). The SPS is based on the assumption that current policies and the EU's existing policy intentions and targets will remain in place. The APS includes advanced economies with net zero emissions pledges, encompassing all Organisation for Economic Co-operation Development countries, except for Mexico, whereas the NZES includes all regions with net zero emissions pledges by 2050. Figure 6 illustrates these scenarios, with values for other years obtained through interpolation.

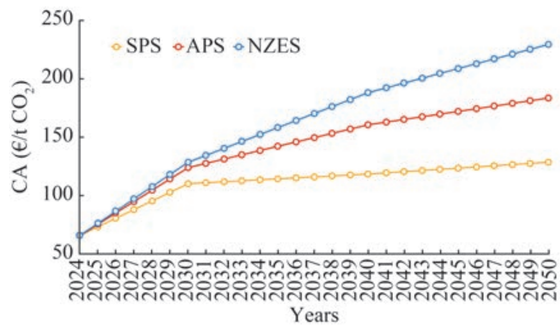

Figure 6 Carbon pricing scenarios

2.5 Limitations and assumptions

The limitations and assumptions of this study are as follows:

1) Within the LCA and LCCA, the system boundaries are placed on the ship's power system rather than on the ship itself. Nevertheless, this approach provides reliable insights into the CF of a ship powered by different fuels, as demonstrated in a study conducted by Bellot et al. (2024). The researchers investigated the CF of a container ship in its various phases, including building, scrapping, and operation. Their findings indicated that 98% of the CF can be attributed to FC.

2) The calculated CF is exclusive to CO_2 and CH_4 emissions, with N_2O emissions excluded because the specific N_2O emissions cannot be isolated from the aggregate NO_x emissions calculated within the model.

3) In the simulation of engine operation, only the main

engine is considered. However, for the calculation of absolute emissions, both the main and auxiliary engines must be taken into account.

4) In the absence of data on the prices of LNG in Croatia, these prices have been estimated based on historical data on the prices of natural gas for non-household consumers, the costs of liquefaction, and the costs of transportation.

3 Results and discussion

3.1 Diesel engine performance under steady operating conditions

The 1D/0D simulation model of the diesel engine of a fishing vessel was validated under steady operating conditions defined by the engine manufacturer. Four engine operating points representing load sweep (i.e., 25%, 50%, 75%, and 100%) at a constant engine speed of 1 500 r/min were considered, and the engine performance and FC were compared with the reference data.

The validation results of engine torque (top diagram) and BSFC (bottom diagram) for load sweep are plotted in Figure 7. During the model calibration, the maximum boost pressure at 100% of the engine load was set to 2.15 bar according to reference engine performance data. The measured BSFC defined by the engine manufacturer is based on ISO 3046/1, including the reference conditions and methods for internal combustion engine performance declaration. The heat transfer calibration factor at each cylinder was reduced from the default unit value to 0.8 so that the maximum difference between measured and simulated BSFC is equal to −3%. The calibration of the simulation model parameters resulted in a single set of parameters without any requirements for case-by-case tuning. Bearing in mind that the load of the engine of a fishing vessel does not exceed 80% during usual operational profiles, the simulation model matched the engine performance and FC under steady operating conditions.

3.2 Fishing vessel performance over the real operating regime

After the calibration of the simulation model under steady operating conditions, the simulation model is extended to transient engine operation, which includes the addition of a vehicle element (V1 shown in Figure 3) that is connected to the engine element. The instantaneous load force that defines the required engine torque is described by the second-degree polynomial function that depends on the instantaneous vessel speed. The desired fishing vessel speed (a result of GPS tracking) is imposed on the simulation model via the vehicle element. Control of the engine load is performed with an ECU element controlling the amount of fuel that will be delivered to each cylinder per operating cycle.

Transient engine operation was simulated for two operating periods of the fishing vessel, as listed in Table 4. The

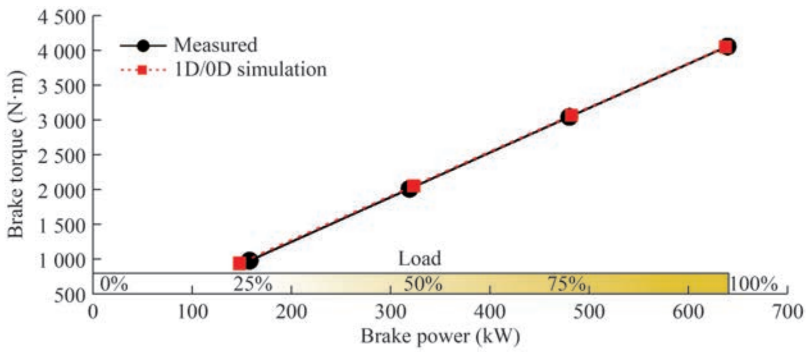

(a) Comparisons of brake torque

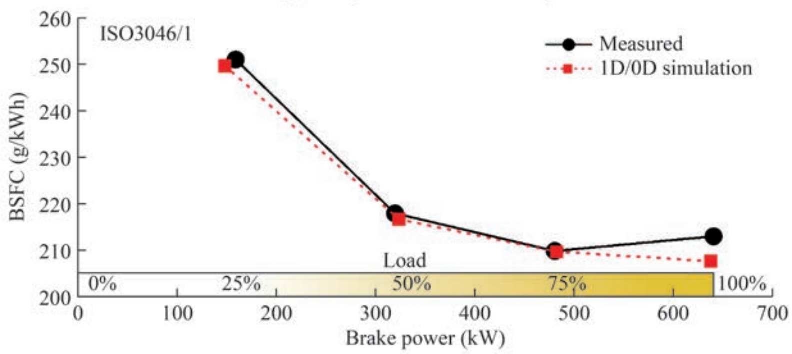

(b) Comparisons of brake specific fuel consumption (BSFC)

Figure 7 Validation results for load sweep (from 25% to 100%) at a constant engine speed of 1 500 r/min first operating period lasts 250 min, whereas the second operating period lasts 43 min, which results in the total operating period of 293 min that is analyzed in this study. Both operating periods have an average vessel speed of approximately 13–14 km/h. The average vessel speed of the simulation model matched the measured data with a maximum difference of 4.4% in the case of dual-fuel engines, as shown in Table 4.

Table 4 Overview of the analyzed operating periods and comparisons of the measured and simulated averaged speeds

Operating period	Operating time (min)	Averaged speed (km/h)		
		Measured	Sim. Diesel	Sim. Dual Fuel
Operating period 1	250	14.4	14.40 (0%)	14.46 (+0.42%)
Operating period 2	43	12.9	13.28 (+2.94%)	13.24 (+2.63%)

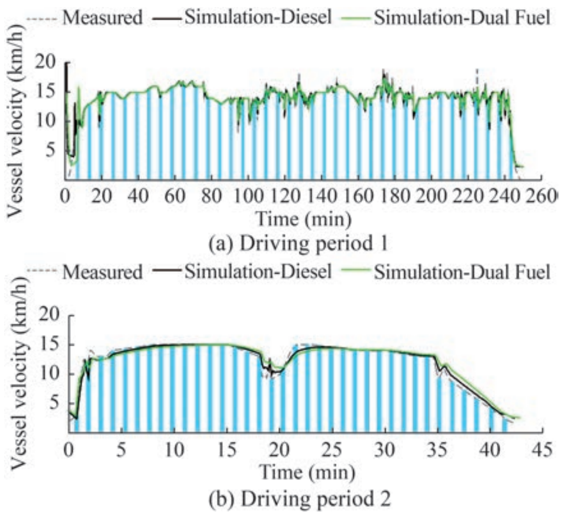

Figure 8 Comparisons of the measured and simulated vessel velocities over two operating periods during the fishing cycle

The comparisons of the measured and simulated vessel speeds of the considered operating periods are given in Figure 8. The simulation model does not accurately reflect the initial operation of the fishing vessel (first 2–3 min), which is attributed to the time required for the speed control gains to be adopted in the ECU element. However, this initial period is relatively brief compared with the total operating time. At the remaining time of the operating periods, the simulation model correctly keeps track of the desired vessel speed. The fuel consumed is integrated over time and further used for the calculation of CO_2 emission for the total operating period.

The final results of the simulation of the two operating periods are presented in Table 5, which shows the FC and investigated tailpipe emissions for different power systems on board the investigated fishing vessel. The higher LHV of dual fuel resulted in FC lower than that of diesel.

To gain insights into the environmental impact of the two power system configurations under investigation, an LCA was conducted, and the results are presented in Figure 9. In the results, D denotes the diesel-powered vessel, whereas LNG85, LNG90, and LNG95 denote the power systems in which LNG comprises 85%, 90%, and 95% of the fuel share, respectively.

As presented in Figure 9, replacing the diesel power system with LNG configurations results in a 14% to 16% reduction in CO_2-eq emissions. Among the configurations considered, LNG95 emerges as the most environmentally friendly option. This finding is attributed to the low proportion of diesel used as a pilot fuel, which constitutes only 5% of the fuel mix. Although this power system emits CH_4 emissions that contribute to global warming, its WTT emissions are lower than those of a diesel power system, and the overall CF is consequently reduced.

To ascertain whether the LNG power system is a more cost-effective option than a diesel power system, an LCCA is conducted. Within the analysis, the investment and maintenance costs are calculated based on the current prices obtained from the literature. The carbon tax is calculated following the most rigorous scenario, which predicts the CA value of 230 €/t CO_2 by 2050 (NZES). The fuel cost is calculated with future fuel prices predicted by Monte Carlo simulations. The results of these simulations are presented in Figure 10 and 11, which illustrates the distributions of 1 000 simulated fuel prices per simulation of each fuel, maintaining consistent statistical properties (mean and StDev). The figures show the results of four simulations. The red line on each histogram denotes a normal distribution curve with the same mean and StDev overlaid for visual reference, indicating the close approximation of the simulated data to a normal distribution.

The results of the Monte Carlo simulations of the price of LNG are calculated to obtain a mean of 0.75 €/kg and StDev of 0.18, whereas those of diesel are calculated to

Table 5 Fuel consumption and emissions on a typical fishing cycle with an operating period of 293 min

Operational fuel consumption and emissions	Powering options			
	Diesel	85% LNG + 15% diesel	90% LNG + 10% diesel	95% LNG + 5% diesel
FC (kg)	213.78	197.22	194.94	193.52
CO_2 emission (kg)	676.08	551.17	541.59	534.45
CH_4 emission (kg)	0	0.776	0.828	0.873

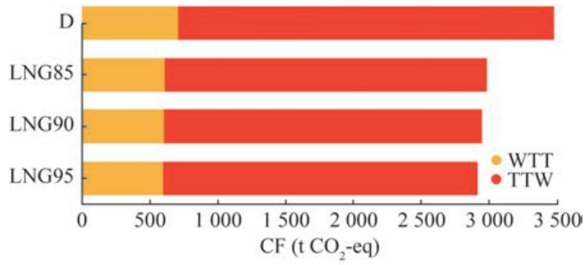

Figure 9 LCA results

obtain a mean of 1.55 €/kg and StDev of 0.22, as shown in Figures 10 and 11. The *x*-axis shows the price of each fuel, which ranges from 0 €/kg to 1.4 €/kg for LNG and ranges from 0 €/kg to 2.3 €/kg for diesel. The *y*-axis shows the frequency of occurrence of each price range in the simulation. The results show that the peak values cluster around the mean and that the distribution reflects the results with minor disturbances.

Although all histograms exhibit a certain degree of alignment with the normal curve, notable discrepancies are evident in terms of skewness and dispersion but are not significant enough to disregard the mean as a reliable indicator of future LNG and diesel prices. Therefore, the prices of 1.55 €/kg for diesel and 0.75 €/kg for LNG are used for the LCCA comparison presented in Figure 12.

The LCCA comparison of diesel and LNG power systems showed that LNG power systems are less expensive than diesel power systems in terms of total costs. Specifi-

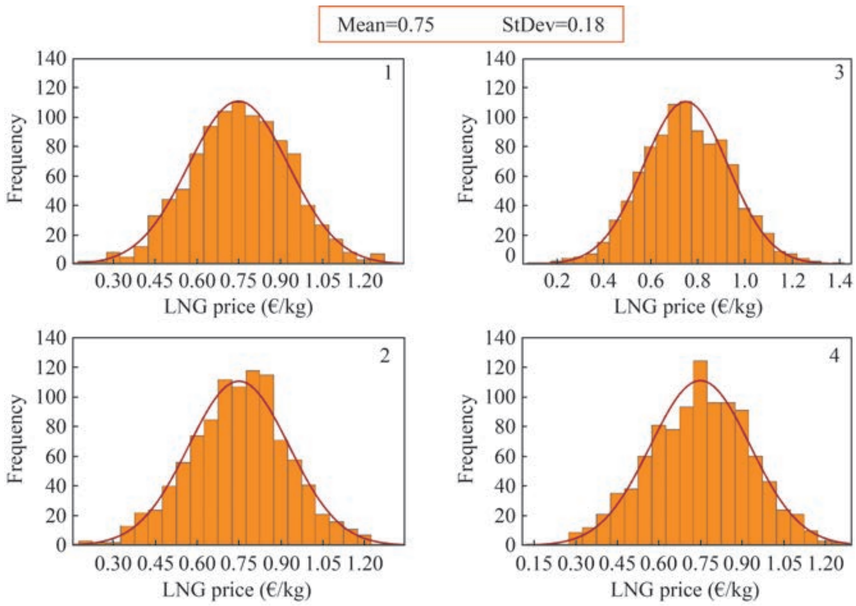

Figure 10 Monte Carlo simulations of LNG prices

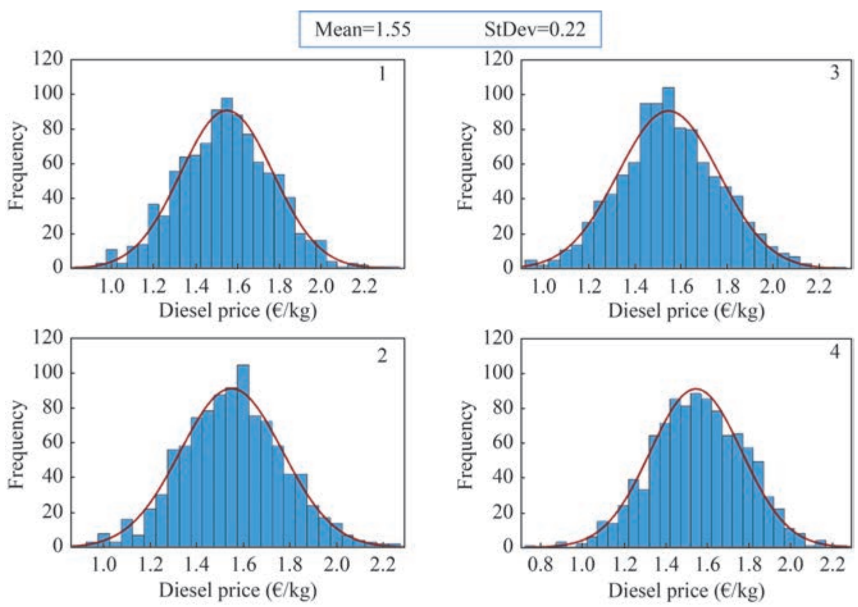

Figure 11 Monte Carlo simulations of diesel prices

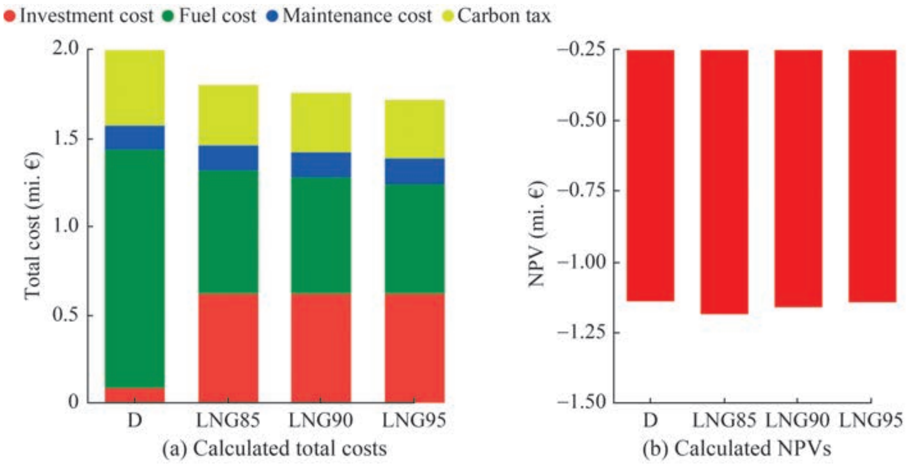

Figure 12 LCCA results

cally, the LNG95 power system configuration achieves the lowest costs, with a 13.8% reduction, whereas LNG85 and LNG90 power system configurations result in 9.5% and 11.8% lower total costs, respectively, which is primarily attributed to the higher costs of diesel fuel and carbon tax. However, the NPV calculation yields a different result. The NPV of the diesel power system is 1.9% and 3.7% lower than that of the LNG power system in the case of LNG90 and LNG85, respectively. By contrast, the NPV of LNG95 is nearly identical to that of the diesel power system, with a difference of only 0.2%. This discrepancy is largely attributed to the higher initial investment cost of LNG-powered ships. In contrast to the costs of diesel fuel and carbon tax, which are discounted over time, the substantial upfront investment cost of LNG infrastructure on board does not benefit from discounting, leading to a higher NPV for LNG systems.

To emphasize the approach of simulating real engine operations during a typical fishing cycle to determine the actual FC and CF of a vessel, this study compares these findings with calculations from a previous study conducted by Perčić et al. (2023b), in which the main engine was assumed to operate at a constant load of 56%. Meanwhile, FC was calculated by multiplying the calculated main engine power, operational time (800 h/year for the main engine), and a fixed specific FC value, i.e., 190 g/kWh for diesel and 160 g/kWh for LNG. Although the previous methodology included the auxiliary engine of the purse seiner, it is excluded from the current comparison for consistency. The FC is evaluated on an annual basis and specifically for the fishing cycle observed in this study. This comparison is conducted for both diesel and investigated LNG power system configurations, with the results presented in Table 6.

The comparison shows that the previous approach to FC calculations for ships resulted in higher values, but not significantly, than the new approach, i.e., approximately 12% to 14% higher.

Table 6 FC calculations for the diesel and LNG power system configurations

kg

Fuel consumption		New approach (simulation of real engine operation)	Previous approach (fixed specific fuel consumption variables)
FC_A	D	35 021.98	40 857.60
	LNG95	31 702.94	36 771.84
	LNG90	31 935.56	36 986.88
	LNG85	32 309.08	37 201.92
FC cycle	D	213.78	249.38
	LNG95	193.52	222.15
	LNG90	194.94	223.45
	LNG85	197.22	224.75

4 Conclusions

This study investigated the proposed replacement of a diesel power system with an LNG power system on board a Croatian fishing vessel (purse seiner) from the environmental and economic points of view by simulating real engine operations during its typical fishing cycle achieved by a 1D/0D simulation model of AVL Boost™, which utilizes real-time data obtained from a monitoring system installed on several Croatian fishing vessels, including the one observed. The results of the simulations are presented in terms of FC and emissions, which are used as a basis for further investigation into the CF of power systems through the life cycle perspective and achieved by conducting a comprehensive LCA. In addition, an LCCA was conducted to assess the economic viability of replacing the power system of a ship with an LNG-based configuration. Monte Carlo simulations were employed to predict future fuel prices, providing a robust analysis of the profitability of such a replacement. The main findings of the research are summarized as follows:

1) Simulations of the real operation of the main engine

indicated the real environmental footprint and FC during its typical fishing cycle.

2) LCA was conducted to investigate the environmental impact of ship power systems, focusing on two important phases, namely WTT and TTW. The WTT emissions were derived using the GREET software, whereas the TTW emissions were calculated using the AVL Boost™ model. The LCA showed that the LNG power systems exhibited a 14% to 16% lower CF than the diesel power system, indicating its potential as a fuel for low-carbon shipping.

3) Monte Carlo simulations were employed to predict future fuel prices of LNG and diesel. Although some discrepancies are evident between the simulated price values and the normal distribution curve, the peak values cluster around the mean, with diesel prices reaching 1.55 €/kg and LNG prices reaching 0.75 €/kg. However, the StDev of the simulated values reflects the potential variability in future prices because of market, political, or other influences.

4) The LCCA comparison of diesel and LNG power systems shows that LNG power systems are more cost-effective than diesel power systems in terms of total costs. Among the configurations analyzed, the LNG95 power system configuration achieves the highest cost reduction of 13.8%, whereas the LNG85 and LNG90 power system configurations show reductions of 9.5% and 11.8%, respectively. These cost advantages are primarily attributed to the higher price of diesel fuel and carbon tax. However, the NPV analysis shows a different outcome. The NPV of the diesel power system is 9% lower than that of the LNG power systems overall. Specifically, the NPV of diesel is 1.9% lower than that of LNG90 and 3.7% lower than that of LNG85. By contrast, LNG95 exhibits an NPV that is nearly identical to that of the diesel power system, with a minimal difference of only 0.2%.

This study emphasizes the necessity of integrating advanced simulation techniques and economic analysis in the pursuit of sustainable and economically viable maritime operations. Although LNG represents an environmentally friendly option, it does not reduce GHG emissions in the substantial manner that is required by the IMO at a lower cost. Therefore, further research will focus on other fuels, such as methanol, with the aforementioned model for simulating real engine operations. In addition, a set of different emissions released during the operation of a ship should be investigated to indicate the real environmental footprint of different power systems.

Nomenclature

Variables

α	Crank angle (°)
BSFC	Brake-specific fuel consumption (g/kWh)
CA	Carbon allowance (€/t CO_2)
CapEx	Capital costs (€)
E	Emission (kg)
FC	Fuel consumption (kg)
GWP	Global warming potential (kg CO_2-eq)
h	Specific enthalpy (J/kg)
LHV	Low heating value (MJ/kg)
m	mass (kg)
n	Time of the lifetime of a ship (year)
NPV	Net present value (€)
OpEx	Operating costs (€)
p	Pressure (Pa)
q	Specific heat (J/kg)
r	Discount rate (%)
u	Specific internal energy (J/kg)
V	Volume (m^3)
x	Mass ratio of burned fuel

Subscripts

A	Annual
BB	Blow-by
C	Cylinder
comb	Combustion
e	Exhaust
ev	Evaporation
f	Fuel
i	Intake
j	Emission

Abbreviations

0D	Zero-dimensional
1D	One-dimensional
A2F	Air to fuel
APS	Announced pledges scenario
CF	Carbon footprint
CO	Intercooler element
E	Engine element
ECU	Engine control unit
EIAPP	Engine International Air Pollution Prevention
ETS	Emission trading system
GHG	Greenhouse gases
GT	Gross tonnage
HFO	Heavy fuel oil
IMO	International Maritime Organization
LCA	Life cycle assessment
LCCA	Life cycle cost assessment
LNG	Liquefied natural gas
MDO	Marine diesel oil
NZES	Net zero emissions by 2050 scenario
SB	System boundary
SPS	Stated policies scenario
StDev	Standard deviation
TC	Turbocharger
TTW	Tank-to-wake
V	Vehicle element
WTT	Well-to-tank

Competing interest The authors have no competing interests to declare that are relevant to the content of this article.

References

Ammar NR (2019) An environmental and economic analysis of methanol fuel for a cellular container ship. Transp. Res. D Transp. Environ. 69: 66-76. https://doi.org/10.1016/j.trd.2019.02.001

Ančić I, Perčić M, Vladimir N (2020) Alternative power options to reduce carbon footprint of ro-ro passenger fleet: A case study of Croatia. J. Clean Prod. 271: 122638. https://doi.org/10.1016/j.jclepro.2020.122638

AVL Boost (2013) User guide, "AVL homepage". Available from https://www.avl.com/simulation [Accessed on Jan. 03, 2025]

Baiju MV, Madhu VR, Dhiju Das PH, Vipin Kumar V, Sajeev N, Nilender K, Upinder K, Veerasamy M (2024) Evaluating LNG-diesel dual-fuel systems in trawling: Results from trials off Cochin, Kerala. Fishery Technology 61: 215-221. https://doi.org/10.56093/ft.v61i3.149805

Basurko OC, Gabiña G, Quincoces I (2016) Fuel consumption monitoring in fishing vessels and its potential for different stakeholders. Available from https://conferences.ncl.ac.uk/media/sites/conferencewebsites/scc2016/1.1.2. pdf [Accessed on Aug. 26, 2023]

Bayraktar M (2023) Investigation of alternative fuelled marine diesel engines and waste heat recovery system utilization on the oil tanker for upcoming regulations and carbon tax. Ocean Engineering 287: 115831. https://doi.org/10.1016/j.oceaneng.2023.115831

Bellér G, Árpád I, Kiss JT, Kocsis D (2021) AVL Boost: a powerful tool for research and education. J. Phys. Conf. Ser. 1935: 012015. https://doi.org/10.1088/1742-6596/1935/1/012015

Bellot A, Baumler R, Bouallou C, Nemer M, Ölcer A (2024) A cradle-to-grave assessment of carbon and energy footprints of ships using synthetic fuel for net-zeros operations. Ocean Engineering 310: 118392. https://doi.org/10.1016/j.oceaneng.2024.118392

Bilgili L (2021) Comparative assessment of alternative marine fuels in life cycle perspective. Renewable and Sustainable Energy Reviews 144: 110985. https://doi.org/10.1016/J.RSER.2021.110985

Blanco-Davis E, Zhou P (2014) LCA as a tool to aid in the selection of retrofitting alternatives. Ocean Engineering 77: 33-41. https://doi.org/10.1016/J.OCEANENG.2013.12.010

Bouman EA, Lindstad E, Rialland AI, Strømman AH (2017) State-of-the-art technologies, measures, and potential for reducing GHG emissions from shipping-A review. Transp. Res. D Transp. Environ. 52: 408-421. https://doi.org/10.1016/j.trd.2017.03.022

Bui KQ, Perera LP, Emblemsvåg J (2022) Life-cycle cost analysis of an innovative marine dual-fuel engine under uncertainties. J. Clean Prod. 380: 134847. https://doi.org/10.1016/j.jclepro.2022.134847

Butarbutar R, Gurning ROS, Semin (2023) Prospect of LNG as marine fuel in Indonesia: An economic review for a case study of 600 TEU container vessel. Applied Sciences 13(5): 2760. https://doi.org/10.3390/app13052760

Colantoni A, Villarini M, Monarca D, Carlini M, Mosconi EM, Bocci E, Rajabi Hamedani S (2021) Economic analysis and risk assessment of biomass gasification CHP systems of different sizes through Monte Carlo simulation. Energy Reports 7: 1954-1961. https://doi.org/10.1016/j.egyr.2021.03.028

DNV (2023) Maritime decarbonization efforts propelled as orders for alternative-fueled vessels grow. Available from https://www.dnv.com/news/maritime-decarbonization-efforts-propelled-as-orders-for-alternative-fueled-vessels-grow-251921/ [Accessed on Jun. 27, 2024]

Duppati G, Younes BZ, Tiwari AK, Hunjra AI (2023) Time-varying effects of fuel prices on stock market returns during COVID-19 outbreak. Resources Policy 81: 103317. https://doi.org/10.1016/j.resourpol.2023.103317

European Commission (2024) Reducing emissions from the shipping sector. Available from https://climate.ec.europa.eu/eu-action/transport/reducing-emissions-shipping-sector_en [Accessed on May 17, 2024]

Eurostat (2024) Natural gas prices- Croatia. Available from https://ec.europa.eu/eurostat/databrowser/view/ten00118/default/table?lang=en [Accessed on Jul. 19, 2024]

FAO (2021) Review of the techno-economic performance of the main global fishing fleets. Available from https://openknowledge.fao.org/server/api/core/bitstreams/5ca84ab9-ee4c-46e3-b4dd-764b6dd44f17/content [Accessed on Jan. 4, 2025]

Ghorbani M, Slaets P, Lacey J (2023) A numerical simulation tool for a wind-assisted vessel verified with logged data at sea. Ocean Engineering 290: 116319. https://doi.org/10.1016/j.oceaneng.2023.116319

GREET (2022) LCA software. Available from https://greet.es.anl.gov/index.php [Accessed on Sep. 27, 2023]

Guo B, Liang Q, Tvete HA, Brinks H, Vanem E (2022) Combined machine learning and physics-based models for estimating fuel consumption of cargo ships. Ocean Engineering 255: 111435. https://doi.org/10.1016/j.oceaneng.2022.111435

Ha S, Jeong B, Jang H, Park C, Ku B (2023) A framework for determining the life cycle GHG emissions of fossil marine fuels in countries reliant on imported energy through maritime transportation: A case study of South Korea. Science of the Total Environment 897: 165366. https://doi.org/10.1016/j.scitotenv.2023.165366

Huang J, Fan H, Xu X, Liu Z (2022) Life cycle greenhouse gas emission assessment for using alternative marine fuels: A very large crude carrier (VLCC) case study. J. Mar. Sci. Eng. 10: 1969. https://doi.org/10.3390/jmse10121969

Hulskotte JHJ, Denier van der Gon HAC (2010) Fuel consumption and associated emissions from seagoing ships at berth derived from an on-board survey. Atmos. Environ. 44: 1229-1236. https://doi.org/10.1016/j.atmosenv.2009.10.018

Iannaccone T, Landucci G, Tugnoli A, Salzano E, Cozzani V (2020) Sustainability of cruise ship fuel systems: Comparison among LNG and diesel technologies. J. Clean Prod. 260: 121069. https://doi.org/10.1016/j.jclepro.2020.121069

IMO (2020) Fourth IMO GHG study. Available from https://safety4sea.com/wp-content/uploads/2020/08/MEPC-75-7-15-Fourth-IMO-GHG-Study-2020-Final-report-Secretariat. pdf [Accessed on Jan. 14, 2024]

IMO (2023) Strategy on reduction of GHG emissions from ships. Available from https://www. imo. org/en/OurWork/Environment/Pages/2023-IMO-Strategy-on-Reduction-of-GHG-Emissions-from-Ships.aspx [Accessed on Jan. 4, 2025]

International Energy Agency (2023) World energy outlook 2023. Available from https://www. iea. org/reports/world-energy-outlook-2023 [Accessed on Jan. 4, 2025]

Jang H, Jeong B, Zhou P, Ha S, Nam D (2021) Demystifying the lifecycle environmental benefits and harms of LNG as marine fuel. Appl. Energy 292: 116869. https://doi.org/10.1016/j.apenergy.2021.116869

Jang J, Lim S, Choe SB, Kim JS, Lim HK, Oh J, Oh D (2024) Enhanced predictive modeling vs. LCA simulation: A comparative study on CO_2 emissions from ship operations. Ocean Engineering 310: 118506. https://doi.org/10.1016/j.oceaneng.2024.118506

Jeong S, Woo JH, Oh D (2020) Simulation of greenhouse gas emissions of small ships considering operating conditions for environmental performance evaluation. International Journal of Naval Architecture and Ocean Engineering 12: 636-643. https://doi.org/10.1016/j.ijnaoe.2020.07.006

Jovanović I, Vladimir N, Perčić M, Koričan M (2022) The feasibility of autonomous low-emission ro-ro passenger shipping in the Adriatic Sea. Ocean Engineering 247: 110712. https://doi.org/10.1016/J.OCEANENG.2022.110712

Karatug C, Arslanoglu Y, Guedes Soares C (2022) Evaluation of decarbonization strategies for existing ships. In: Trends in Maritime Technology and Engineering Volume 2, CRC Press, London, 45-54

Karatuğ Ç, Ceylan BO, Ejder E, Arslanoğlu Y (2023a) Investigation and examination of LNG, methanol, and ammonia usage on marine vessels. In: Zincir B, Shukla PC, Agarwal AK (Eds.). Decarbonization of Maritime Transport. Energy, Environment, and Sustainability, Springer, Singapore, 65-85. https://doi.org/10.1007/978-981-99-1677-1_5

Karatuğ Ç, Ejder E, Tadros M, Arslanoğlu Y (2023b) Environmental and economic evaluation of dual-fuel engine investment of a container ship. Journal of Marine Science and Application 22: 823-836. https://doi.org/10.1007/s11804-023-00381-3

Karatuğ Ç, Tadros M, Ventura M, Guedes Soares C (2024) Decision support system for ship energy efficiency management based on an optimization model. Energy 292: 130318. https://doi.org/10.1016/j.energy.2024.130318

Kim JK, Jeong B, Choi JH, Lee WJ (2023) Life cycle assessment of LPG engines for small fishing vessels and the applications of bio LPG fuel in Korea. J. Mar. Sci. Eng. 11: 1488. https://doi.org/10.3390/jmse11081488

Kjær LL, Pagoropoulos A, Hauschild M, Birkved M, Schmidt JH, McAloone TC (2015) From LCC to LCA using a hybrid Input Output model-a maritime case study. Procedia CIRP 29: 474-479. https://doi.org/10.1016/J.PROCIR.2015.02.004

Korberg AD, Brynolf S, Grahn M, Skov IR (2021) Techno-economic assessment of advanced fuels and propulsion systems in future fossil-free ships. Renewable and Sustainable Energy Reviews 142: 110861. https://doi.org/10.1016/J.RSER.2021.110861

Koričan M, Perčić M, Vladimir N, Alujević N, Fan A (2022) Alternative power options for improvement of the environmental friendliness of fishing trawlers. J. Mar. Sci. Eng. 10: 1882. https://doi.org/10.3390/jmse10121882

Koričan M, Vladimir N, Fan A (2023) Investigation of the energy efficiency of fishing vessels: Case study of the fishing fleet in the Adriatic Sea. Ocean Engineering 286: 115734. https://doi.org/10.1016/j.oceaneng.2023.115734

Kumar S, Kwon HT, Choi KH, Lim W, Cho JH, Tak K, Moon I (2011) LNG: An eco-friendly cryogenic fuel for sustainable development. Appl Energy 88: 4264-4273

Lee H, Lee J, Roh G, Lee S, Choung C, Kang H (2024) Comparative life cycle assessments and economic analyses of alternative marine fuels: Insights for practical strategies. Sustainability 16: 2114. https://doi.org/10.3390/su16052114

Lindstad E, Lagemann B, Rialland A, Gamlem GM, Valland A (2021) Reduction of maritime GHG emissions and the potential role of E-fuels. Transp. Res. D Transp. Environ. 101: 103075. https://doi.org/10.1016/J.TRD.2021.103075

Liu Y, Ge Y, Tan J, Fu M, Shah AN, Li L, Ji Z, Ding Y (2018) Emission characteristics of offshore fishing ships in the Yellow Bo Sea, China. Journal of Environmental Sciences 65: 83-91. https://doi.org/10.1016/j.jes.2017.02.020

MAPON (2024) Fleet management & asset tracking platform. Available from https://www. mapon. com/en [Accessed on Jun. 14, 2024]

Ministry of Agriculture of Republic of Croatia (2023) Fishing vessel particulars. Directory of Fisheries. Available from https://ribarstvo.mps.hr/default.aspx?id=13 [Accessed on Aug. 29, 2023]

Mishra P, Pandey C, Singh U, Gupta A, Sahu C, Keshri A (2019) Descriptive statistics and normality tests for statistical data. Ann Card Anaesth. 22: 67-72. https://doi.org/10.4103/aca.ACA_157_18

Perčić M, Ančić I, Vladimir N (2020a) Life-cycle cost assessments of different power system configurations to reduce the carbon footprint in the Croatian short-sea shipping sector. Renewable and Sustainable Energy Reviews 131: 110028. https://doi.org/10.1016/j.rser.2020.110028

Perčić M, Koričan M, Jovanović I, Vladimir N (2023a) Environmental and economic assessment of batteries for marine applications: Case study of all-electric fishing vessels. Batteries 10: 7. https://doi.org/10.3390/batteries10010007

Perčić M, Vladimir N, Fan A (2020b) Life-cycle cost assessment of alternative marine fuels to reduce the carbon footprint in short-sea shipping: A case study of Croatia. Appl. Energy 279: 115848. https://doi.org/10.1016/j.apenergy.2020.115848

Perčić M, Vladimir N, Fan A (2021) Techno-economic assessment of alternative marine fuels for inland shipping in Croatia. Renewable and Sustainable Energy Reviews 148: 111363. https://doi.org/10.1016/J.RSER.2021.111363

Perčić M, Vladimir N, Jovanović I, Koričan M (2022) Application of fuel cells with zero-carbon fuels in short-sea shipping. Appl. Energy 309: 118463. https://doi. org/10.1016/J. APENERGY. 2021.118463

Perčić M, Vladimir N, Koričan M, Jovanović I, Haramina T (2023b) Alternative fuels for the marine sector and their applicability for purse seiners in a life-cycle framework. Applied Sciences 13: 13068. https://doi.org/10.3390/app132413068

Qu J, Feng Y, Zhu Y, Wu B, Wu Y, Xiao Z, Zheng S (2023) Assessment of a methanol-fueled integrated hybrid power system of solid oxide fuel cell and low-speed two-stroke engine for maritime application. Appl. Therm. Eng. 230: 120735. https://doi.org/10.1016/j.applthermaleng.2023.120735

Sjerić M, Tomić R, Martić I, Degiuli N, Grlj CG (2024) Environmental and economic aspects of a containership engine performance in off-design conditions. Applied Sciences 14: 4634. https://doi.org/10.3390/app14114634

Statista (2024) Diesel price in Croatia. Available from https://www.statista.com/statistics/603784/diesel-fuel-prices-croatia/ [Accessed on Jul. 18, 2024]

Szelangiewicz T, Abramowski T, Żelazny K, Sugalski K (2021) Reduction of resistance, fuel consumption and GHG emission of a small fishing vessel by adding a bulbous bow. Energies 14(7): 1837. https://doi.org/10.3390/en14071837

Taghavifar H (2023) Experimental and numerical engine cycle setup for a dual fuel hydrogen, methane, and hythane with diesel to assess the effect of water injection and nozzle geometry. Environ. Prog. Sustain. Energy 42(1): e13936. https://doi.org/10.1002/ep.13936

Taghavifar H, Mazari F (2022) 1D diesel engine cycle modeling integrated with MOPSO optimization for improved NO_x control and pressure boost. Energy 247: 123517. https://doi.org/10.1016/j.energy.2022.123517

Taghavifar H, Perera LP (2023a) The effect of LNG and diesel fuel emissions of marine engines on GHG-reduction revenue policies under life-cycle costing analysis in shipping. Proceedings of the ASME 2023 42nd International Conference on Ocean, Offshore and Arctic Engineering. Volume 5: Ocean Engineering, Melbourne, Australia, V005T06A035. https://doi.org/10.1115/OMAE2023-104508

Taghavifar H, Perera LP (2023b) Life cycle emission and cost assessment for LNG-retrofitted vessels: the risk and sensitivity analyses under fuel property and load variations. Ocean Engineering 282: 114940. https://doi.org/10.1016/j.oceaneng.2023.114940

Theotokatos G, Stoumpos S, Bolbot V, Boulougouris E (2020) Simulation-based investigation of a marine dual-fuel engine. Journal of Marine Engineering & Technology 19: 5-16. https://doi.org/10.1080/20464177.2020.1717266

Tomos BAD, Stamford L, Welfle A, Larkin A (2024) Decarbonising international shipping-A life cycle perspective on alternative fuel options. Energy Convers. Manag. 299: 117848. https://doi.org/10.1016/j.enconman.2023.117848

Tools (2024) Diesel price in Croatia. Available from https://www.tolls.eu/fuel-prices [Accessed on Jul.18, 2024]

Trading Economics (2024a) Croatia—Natural gas prices: Non-household consumers. Available from https://tradingeconomics.com/croatia/gas-prices-non-household-medium-size-consumers-eurostat-data.html [Accessed on Jul.19, 2024]

Trading Economics (2024b) EU carbon permits. Available from https://tradingeconomics.com/commodity/carbon [Accessed on Jul. 19, 2024]

UNFCCC (2001) Climate change information kit. Available from https://unfccc.int/resource/iuckit/cckit2001en.pdf [Accessed on Jan. 04, 2025]

UNFCCC (2024) The Paris agreement. Available from https://unfccc.int/process-and-meetings/the-paris-agreement/the-paris-agreement [Accessed on Nov. 3, 2024]

Wang H, Boulougouris E, Theotokatos G, Zhou P, Priftis A, Shi G (2021) Life cycle analysis and cost assessment of a battery powered ferry. Ocean Engineering 241: 110029. https://doi.org/10.1016/J.OCEANENG.2021.110029

Wang H, Zhou P, Liang Y, Jeong B, Mesbahi A (2020) Optimization of tugboat propulsion system configurations: A holistic life cycle assessment case study. J. Clean Prod. 259: 120903. https://doi.org/10.1016/j.jclepro.2020.120903

Wu Y, Guo H, Qi J, Wang S, Zhen L (2024) Ship refueling optimization for dual-fuel ships considering carbon intensity indicator rating limit and uncertain fuel prices. Multimodal Transportation 3: 100138. https://doi.org/10.1016/j.multra.2024.100138

Xin R, Zhai J, Liao C, Wang Z, Zhang J, Bazari Z, Ji Y (2022) Simulation study on the performance and emission parameters of a marine diesel engine. J. Mar. Sci. Eng. 10: 985. https://doi.org/10.3390/jmse10070985

Yan X, He Y, Fan A (2023) Carbon footprint prediction considering the evolution of alternative fuels and cargo: A case study of Yangtze River ships. Renewable and Sustainable Energy Reviews 173: 113068. https://doi.org/10.1016/j.rser.2022.113068

Yao S, Li C, Wei Y (2023) Design and optimization of a zero carbon emission system integrated with the utilization of marine engine waste heat and LNG cold energy for LNG-powered ships. Appl. Therm. Eng. 231: 120976. https://doi.org/10.1016/j.applthermaleng.2023.120976

Zhou C, Tang W, Ding Y, Huang H, Xu H (2024) Analysis of carbon emission reduction paths for ships in the Yangtze River: The perspective of alternative fuels. J. Mar. Sci. Eng. 12: 947. https://doi.org/10.3390/jmse12060947

Zincir BA, Arslanoglu Y (2024) Comparative life cycle assessment of alternative marine fuels. Fuel 358: 129995. https://doi.org/10.1016/j.fuel.2023.129995

Zou Q, Yi C, Wang K, Yin X, Zhang Y (2022) Global LNG market: supply-demand and economic analysis. IOP Conf. Ser. Earth Environ. Sci. 983: 012051. https://doi.org/10.1088/1755-1315/983/1/012051